

Antineoplastic activity of linear leucine homodipeptides and their potential mechanisms of action

Yun Lei^a, Xiao-Xia Yang^{b,d}, Wei Guo^b, Fu-yong Zhang^b, Xiao-Jian Liao^b, Hui-Fu Yang^b, Shi-Hai Xu^b and Sheng Xiong^{a,c}

Galaxamide is a rare cyclic homopentapeptide composed of three leucines and two *N*-methyl leucines isolated from marine algae *Galaxaura filamentosa*. The strong antitumor activity of this compound makes it a promising candidate for tumor therapy. The synthesis of galaxamide, however, is a complex process, and it has poor water solubility. On the basis of its special chemical composition, we designed a series of linear leucine homopeptides. Among seven dipeptide derivatives, five compounds with terminal protection groups and methyl substitution of the hydrogen in the amido group showed remarkable inhibitory effects against various cancer cells. *N*-tertbutyl-*D*-leucine-*N*-methyl-*D*-leucinebenzyl (A7), the only stereomer condensed by two *D*-leucines, showed the highest antineoplastic activity. A7-treated cells showed cell cycle arrest and morphological changes typical of cells undergoing apoptosis. The population of Annexin-V positive/propidium iodide-negative cells also increased, indicating the induction of early apoptosis. A7 promoted the cleavage of caspase-9 and caspase-3, as well as increased intracellular Ca²⁺ levels and decreased the mitochondrial membrane potential. Collectively, certain linear leucine dipeptides derived from

cyclic pentapeptide are able to inhibit tumor cell proliferation through cell cycle arrest and apoptosis induction. The *N*-methyl group in the side chain and the *D*/*L* conformation of the amino-acid residue are critical for their activity. *Anti-Cancer Drugs* 00:000–000 Copyright © 2018 Wolters Kluwer Health, Inc. All rights reserved.

Anti-Cancer Drugs 2018, 00:000–000

Keywords: antineoplastic activity, apoptosis, cyclic peptide, homo-oligopeptide, leucine dipeptide

^aDepartment of Cell Biology, Institute of Biomedicine, ^bDepartment of Chemistry, Jinan University, ^cNational Engineering Research Center of Genetic Medicine, Guangzhou and ^dZhaoqing Aquatic Technologies Popolarizing Center, Zhaoqing, People's Republic of China

Correspondence to Sheng Xiong, PhD, Department of Cell Biology, 730 Building of Biology, Jinan University, 601 W Huangpu Avenue, Guangzhou 510632, Guangdong, People's Republic of China
Tel/fax: +86 208 522 2759; e-mail: xsh_jnu@hotmail.com

or

Correspondence to Shi-Hai Xu, PhD, Department of Chemistry, Jinan University, Guangzhou 510632, Guangdong, People's Republic of China
Tel/fax: +86 208 522 8856; e-mail: txush@jnu.edu.cn

Received 3 October 2017 Revised form accepted 12 February 2018

Introduction

Now, therapeutic antibodies have emerged to be the star category of anti-cancer drugs [1]. However, the complex structure and large molecular size make the manufacture and utilization of antibodies difficult. For example, because of their large size, antibodies have a decreased ability to penetrate tissues and cannot pass through the blood–brain barrier. These factors limit their usage in diseases of the central nervous system [2]. Small peptides from natural sources have certain competitive advantages over small-molecule drugs and monoclonal antibodies because of their small size, low toxicity and immunogenicity, strong target specificity, and the relative ease with which they can be modified and designed [3,4]. Thus, they have attracted considerable attention as candidates for cancer therapy.

Small peptides with antineoplastic activity can be found in sources such as terrestrial animals, marine organisms, microorganisms, milk, and eggs. They exert their tumor-inhibitory effects through apoptosis induction,

angiogenesis inhibition, stimulation of immune response, or blocking tumor-related processes such as cell adhesion and metastasis through various pathways [5]. Peptides from natural sources can either serve as therapeutic agents directly or as 'lead' compounds for further modification to improve their therapeutic potential [6]. Efforts have been focused on the artificial synthesis of such peptide-based compounds and development of their derivatives with improved biological activity. Compared with linear counterparts, cyclic peptides have advantages because of their exceptional stability and enhanced activities [7]. However, laboratory synthesis of cyclic peptides is still challenged by several thermodynamic and kinetic issues. Therefore, most peptides are naturally synthesized as linear chains.

Galaxamide is a monocyclic pentapeptide that we first isolated from marine algae *Galaxaura filamentosa*. In a previous study, we designed a retrosynthesis strategy and successfully synthesized this cyclic peptide. An in-vitro cytotoxic assay showed that it was biologically active against the human renal cell carcinoma GRC-1 cells and human hepatocellular carcinoma HepG2 cells, with

Supplemental Digital Content is available for this article. Direct URL citations appear in the printed text and are provided in the HTML and PDF versions of this article on the journal's website, www.anti-cancerdrugs.com.

corresponding IC₅₀ values of 4.26 and 4.63 µg/ml [8]. The antitumor potential of this cyclic pentapeptide makes it a promising candidate for tumor therapy; however, the complex process required for synthesis and the relatively poor water solubility of this compound are limitations. As a rare cyclopeptide, galaxamide is highly symmetric in structure. It is composed of three leucines and two *N*-methyl leucines, which contribute toward its insolubility. On the basis of its chemical composition, we explored the possibility that some linear oligopeptides derived from galaxamide would also be biologically active against tumors while having a smaller molecular size and better water solubility. Following this idea, a series of leucine homo-oligopeptides were synthesized and evaluated. Interestingly, certain leucine homo-oligopeptides including dipeptides, tripeptides, and pentapeptides showed antineoplastic activity. The dipeptides were especially active, and some inhibited tumor cell proliferation to a degree comparable to that of galaxamide in certain tumor cell lines. In this paper, we summarized the synthesis, structure, antineoplastic activity, and potential mechanisms of action of the novel leucine dipeptides.

Materials and methods

Peptide synthesis, purification, and characterization

All reagents were obtained from commercial suppliers and used without further purification, except for the evaporation of methanol, tetrahydrofuran (THF), and dichloromethane. The reactions were carried out under an inert atmosphere of N₂, and the progress of the reaction was monitored by thin-layer chromatography on precoated glass plates (silica gel 60, F254, 0.25 mm, Ocean Chemical Company, Qingdao, China). High-performance liquid chromatography was used to determine the purity of certain compounds. The melting points were measured by a thermometer without calibration. Optical rotations were measured using a Schmidt + Haensch Polartronic D instrument (Schmidt + Haensch, Berlin, Germany). Proton and carbon NMR spectra were recorded on an Inova 500NB: Varian, Palo Alto, California, USA (500 MHz). Liquid chromatography–mass spectrometry (LCMS) of the synthesized compounds was examined on an LCMS-4000 Q TRAP Shimadzu spectrometer (Applied Biosystems, Waltham, Massachusetts, USA) using the electrospray ionization (ESI) mode of ionization. The three-dimensional configuration space of A7 was determined by X-ray crystallography (Smart 1000 CCD; Bruker: Billerica, Massachusetts, USA).

Synthesis of two material segment

N-Me-Boc-Leu (E3)

Hydriodic methane (15 mmol, 3.15 ml) was added to a solution of Boc-L-Leu-OH (10 mmol, 2.31 g) in THF (30 ml) slowly under an ice bath. The mixture was stirred vigorously for 30 min and 60% hydriod sodium (50 mmol, 1.2 g) was added smoothly. The mixture was stirred for 1h more in ice bath, and then be reacted overnight in room temperature. The reaction was cooled in an ice bath

and a saturation aqueous solution of NH₄Cl (10 ml) and saturation NaHCO₃ was added in turn. The THF was evaporated in decompression. The aqueous solution were washed with petroleum ether (2 × 25 ml), 1 mol HCl was added to adjust the pH as 2–3, and extracted with EtOAc (4 × 50 ml). The combined organic layers were washed with sodium thiosulfate (5%, 75 ml) and saturation NaCl (75 ml), dried (Na₂SO₄), filtered, and concentrated. Finally, a 1.99 g product was obtained. Yellow oil, yield 87%, ¹H NMR (400 MHz, CDCl₃) δ (ppm): 4.82 (m, ^{0.5}H), 4.62 (m, ^{0.5}H), 2.80 (s, ³H), 1.71 (m, ²H), 1.58 (m, ¹H), 1.46 (s, ⁹H), 0.95 (d, *J* = 6.4 Hz ⁶H); MS (ESI) *m/z*: 246.2 [M + H]⁺, 263.2 [M + NH₄]⁺, 268.3 [M + Na]⁺.

Leu-OBn (E6)

The reaction was started with L-Leu (30 mmol, 3.9 g), benzyl methanol (45 mmol, 4.8 ml), P-toluenesulfonic acid (36 mmol, 60 g), and toluene (90 ml) and heated to reflux for 4 h, cooled and diluted by aether (80 ml), washed with saturation sodium carbonate (2 × 80 ml), and the aqueous layers were extracted with aether (2 × 80 ml). The combined organic layers were dried (Na₂SO₄), filtered, the solvent was evaporated, and repeated crystal by EtOAc. Finally, 9.76 g L-Leu-OBn·TosOH was obtained, yield 82%, melting point (m.p.): 54–58°C; ¹H NMR (500 MHz, CDCl₃) δ (ppm): 7.77 (d, *J* = 8.1 Hz ²H), 7.33 (m, ⁵H), 7.18 (d, *J* = 8.0 Hz 2H), 5.22 (dd, *J* = 12, 24.3 Hz ²H), 3.84 (m, ¹H), 2.73 (t, *J* = 5.2, ³H), 2.36 (s, ²H), 1.87 (m, ²H), 1.68 (m, ¹H), 0.87 (m, ⁶H).

Synthesis of Leu-Leu dipeptide benzyl ester derivatives Boc-L-Leu-N-Me-L-Leu-OBn (A1)

A reaction mixture containing Boc-L-Leu-OH (4.8 mmol, 1.1 g) in THF (8 ml), DEPBT (6.0 mmol, 1.8 g), and DIEA (6.0 mmol, 1.05 ml) was stirred at 0°C for 5 min. Then, H-*N*-Me-L-Leu-OBn·TosOH (4 mmol, 1.6 g) was added and raised to room temperature naturally and stirred vigorously for 8 h. The solvent was evaporated in decompression. The residue was purified by column chromatography (silica gel, hexane/acetone = 20:1). Finally, a 1.76 g product was obtained. Achromaticity crystalloid, yield 89%, m.p.: 66–68°C; [α]_D24–67 (*c* = 0.19 CH₃OH); ¹H NMR (500 MHz, DMSO) δ (ppm): 7.35 (m, ⁵H), 6.97 (d, *J* = 8.0, ¹H), 5.23 (dd, *J* = 11.3, 3.0 Hz, ¹H), 5.09 (m, ²H), 4.33 (m, ¹H), 2.89 (s, ³H), 1.76 (m, ¹H), 1.58 (m, ²H), 1.45 (m, ¹H), 1.34 (s, ⁹H), 1.20 (m, ²H), 0.93 (m, ¹²H); ¹³C NMR (CDCl₃, 125 Hz) δ (ppm): 173.9, 171.5, 155.7, 135.4, 128.5 (°C), 128.3, 128.0 (°C), 79.4, 66.9, 54.4, 48.9, 41.9, 36.8, 30.7, 28.2 (°C), 24.7, 24.5, 23.3, 23.2, 21.7, 21.3; MS (ESI) *m/z*: 449.3 [M + H]⁺, 466.5 [M + NH₄]⁺, 471.6 [M + Na]⁺.

BOC-N-Me-L-Leu-L-Leu-OBn (A2)

A reaction mixture containing Boc-*N*-Me-L-Leu-OH (6 mmol, 1.47 g) in THF (8 ml), DEPBT (9.0 mmol, 2.69 g), and DIEA (9.0 mmol, 1.6 ml) was stirred at 0°C for 5 min. Then, L-Leu-OBn·TosOH (6.6 mmol, 2.59 g) was added and raised to room temperature naturally and

stirred vigorously for 12 h. The solvent was evaporated in decompression. The residue was purified by column chromatography (silica gel, hexane/acetone = 20:1). Finally, a 2.42 g product was obtained. Achromaticity crystalloid, yield 90%, $[\alpha]_{\text{D}24-64}$ ($c=0.26$, CH₃OH); m.p.: 68–69°C; ¹H NMR (500 MHz, CDCl₃) δ (ppm): 7.36 (m, ⁵H), 6.51 (s, ¹H), 5.16 (m, ²H), 4.65 (s, ²H), 2.75 (s, ³H), 1.63 (m, ⁴H), 1.54 (m, ²H), 1.48 (s, ⁹H), 0.93 (m, ¹²H); MS (ESI) m/z : 449.3 [M + H]⁺, 466.5 [M + NH₄]⁺, 471.6 [M + Na]⁺.

Boc-L-Leu-L-Leu-OBn (A3)

A reaction mixture containing Boc-L-Leu-OH (6.6 mmol, 1.5 g) in THF (10 ml), DEPBT (9.0 mmol, 2.69 g), and DIEA (9.0 mmol, 1.6 ml) was stirred at 0°C for 5 min. Then, L-Leu-OBn·TosOH (6 mmol, 2.4 g) was added and raised to room temperature naturally and stirred vigorously for 6 h. The solvent was evaporated in decompression. The residue was purified by column chromatography (silica gel, hexane/acetone = 20:1). Finally, a 2.47 g product was obtained. Achromaticity crystalloid, yield 92%, $[\alpha]_{\text{D}24-31}$ ($c=0.25$, CH₃OH); m.p.: 86–87°C; ¹H NMR (500 MHz, CDCl₃) δ (ppm): 7.35 (m, ⁵H), 6.40 (d, $J=7.9$ Hz, ¹H), 5.16 (m, ²H), 4.86 (d, $J=7.5$ Hz, ¹H), 4.67 (m, ¹H), 4.09 (s, ¹H), 1.68 (m, ⁴H), 1.56 (m, ²H), 1.44 (s, ⁹H), 0.91 (m, ¹²H) MS (ESI) m/z : 435.3 [M + H]⁺, 452.5 [M + NH₄]⁺, 457.6 [M + Na]⁺.

Boc-D-Leu-N-Me-L-Leu-OBn (A4)

Boc-D-Leu-OH (11 mmol, 2.54 g) was dissolved in dichloromethane (80 mL) in ice bath; HOBt (11 mmol, 1.47 g) and EDCI (11 mmol, 2.10 g) were added in turn, and dripped DIEA (11 mmol, 1.9 ml). After stirring for 20 min, H-N-Me-L-Leu-OBn·TosOH (10 mmol, 4.07 g) was added to the mixture, raised to room temperature naturally, and stirred vigorously for 24 h. The reaction was cooled in an ice bath and a half-saturation aqueous solution of NH₄Cl (3 × 50 ml) was added, washed with saturation brine (50 ml), dried (Na₂SO₄), filtered, and concentrated. The residue was purified by chromatography (silica gel, hexane/acetone = 20:1). Finally, a 3.9 g product was obtained. Achromaticity crystalloid, yield 87%, $[\alpha]_{\text{D}24-7.5}$ ($c=0.21$, CH₃OH); m.p.: 49–49.9°C; ¹H NMR (CDCl₃) δ (ppm): 7.32 (m, ⁵H), 5.24 (d, $J=9.0$ Hz, ¹H), 5.15 (m, ³H), 4.69 (m, ¹H), 2.97 (s, ³H), 1.73 (m, ⁴H), 1.42 (s, ⁹H), 1.37 (m, ²H), 0.92 (m, ¹²H); ¹³C NMR (CDCl₃, 125 Hz), δ (ppm): 173.9 (¹C), 171.3 (¹C), 155.5 (¹C), 135.6 (¹C), 128.7 (¹C), 128.5 (¹C), 128.2 (¹C), 128.0 (²C), 79.4 (¹C), 66.8 (¹C), 55.2 (¹C), 49.14 (¹C), 42.8 (¹C), 37.4 (¹C), 31.6 (¹C), 28.3 (³C), 25.0 (¹C), 24.6 (¹C), 23.3 (¹C), 23.2 (¹C), 21.9 (¹C), 21.3 (¹C). MS (ESI) m/z : 449.3 [M + H]⁺, 466.5 [M + NH₄]⁺, 471.6 [M + Na]⁺.

Boc-L-Leu-N-Me-D-Leu-Obn (A5)

A reaction mixture containing Boc-L-Leu-OH (6.6 mmol, 1.5 g) in THF (10 ml), DEPBT (9.0 mmol, 2.69 g), and DIEA (9.0 mmol, 1.6 ml) was stirred at 0°C for 5 min.

Then, L-Leu-OBn·TosOH (6 mmol, 2.4 g) was added and raised to room temperature naturally and stirred vigorously for 6 h. The solvent was evaporated in decompression. The residue was purified by column chromatography (silica gel, hexane/acetone = 20:1). Finally, a 2.47 g product was obtained. Achromaticity crystalloid, yield 87%, $[\alpha]_{\text{D}24+9.6}$ ($c=0.32$, CH₃OH); m.p.: 51–52°C; ¹H NMR (CDCl₃) δ (ppm): 7.31 (m, ⁵H), 5.25 (d, ¹H), 5.14 (m, ³H), 4.70 (m, ¹H), 2.97 (s, ³H), 1.71 (m, ⁴H), 1.44 (s, ¹¹H), 1.33 (m, ²H), 0.93 (m, ¹²H); ¹³C NMR (CDCl₃) δ (ppm): 173.9 (¹C), 171.5 (¹C), 155.7 (¹C), 135.4 (¹C), 128.5 (¹C), 128.4 (¹C), 128.3 (¹C), 128.2 (²C), 79.4 (¹C), 66.9 (¹C), 54.4 (¹C), 48.9 (¹C), 41.9 (¹C), 36.9 (¹C), 30.8 (¹C), 28.3 (¹C), 28.2 (¹C), 28.2 (¹C), 24.7 (¹C), 24.5 (¹C), 23.3 (¹C), 23.2 (¹C), 21.7 (¹C), 21.3 (¹C). MS (ESI) m/z : 449.3 [M + H]⁺, 466.5 [M + NH₄]⁺, 471.6 [M + Na]⁺.

Boc-N-Me-L-Leu-N-Me-L-Leu-Obn (A6)

A solution of Boc-L-Me-Leu-OH (3.3 mmol, 0.81 g) in THF (5 ml) was prepared under an ice bath, and DEPBT (4.5 mmol, 1.35 g) and DIEA (4.5 mmol, 0.8 ml) were added in turn. After stirring for 5 min, H-N-Me-L-Leu-OBn·TosOH (3 mmol, 1.27 g) was added to the mixture, raised to room temperature naturally, and stirred vigorously for 18 h. The solvent was evaporated in decompression. The residue was purified by column chromatography (silica gel, hexane/acetone = 20:1). Finally, a 1.12 g product was obtained. Achromaticity oil, yield 81%, $[\alpha]_{\text{D}24-109.6}$ ($c=0.7$, CH₃OH); ¹H NMR (CDCl₃) δ (ppm): 7.33 (m, ⁵H), 5.31 (m, ¹H), 5.09 (m, ²H), 4.85 (m, ¹H), 2.83 (s, ³H), 2.70 (s, ³H), 1.70 (m, ⁴H), 1.43 (s, ⁹H), 1.37 (m, ²H), 0.91 (m, ¹²H); MS (ESI) m/z : 463.3 [M + H]⁺, 480.5 [M + NH₄]⁺, 485.6 [M + Na]⁺.

Boc-D-Leu-N-Me-D-Leu-Obn (A7)

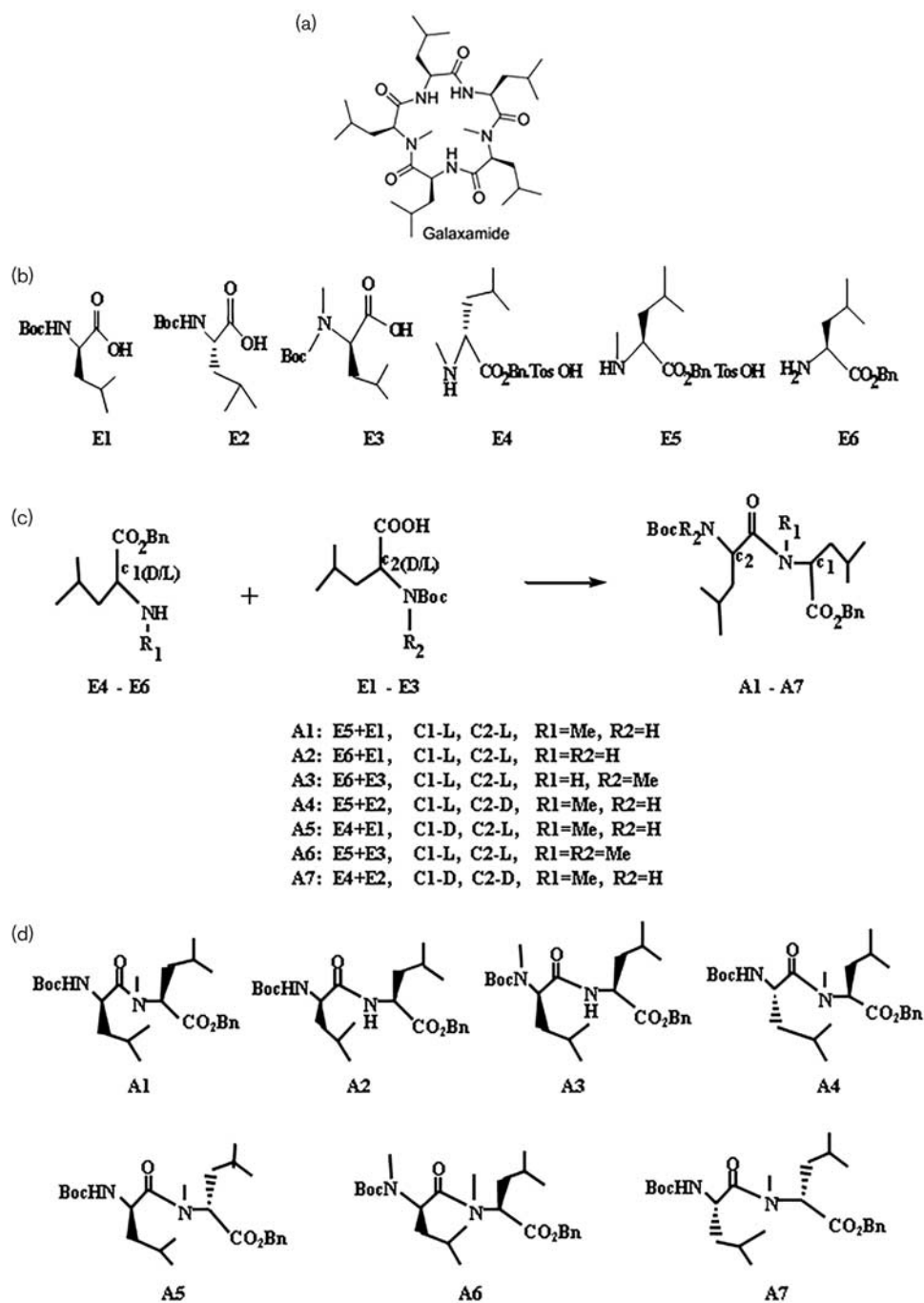
A solution of H-N-Me-D-Leu-OBzl·TosOH (4 mmol, 1.6 g) was prepared in dichloromethane (50 ml) under an ice bath; water (40 ml), Boc-D-Leu-OH (4 mmol, 0.924 g), and HOBt (4 mmol, 0.54 g) were added in turn. The mixture was stirred for 30 min at 0–5°C, EDCI (4.4 mmol, 0.84 g) was added, and stirred for another 24 h at 0–5°C. Then, a diluted aqueous solution of HCl (0.5 mol, 20 ml) was added. The organic and the aqueous layers were separated and the latter were extracted with EtOAc (3 × 3 ml). The combined organic layers were washed with saturation NaHCO₃ three times and saturation citric acid two times, and then washed to litmusless pH by saturation NaCl, dried (Na₂SO₄), filtered, and concentrated. The residue was purified by chromatography (silica gel, hexane/acetone = 30:1). Finally, a 1.54 g product was obtained. Achromaticity crystalloid, yield 86%, $[\alpha]_{\text{D}20-0.70}$ ($c=0.2$ CH₃OH); m.p.: 49–49.9°C. ¹H NMR (DMSO) δ (ppm): 7.35 (m, ⁵H), 6.94 (d, $J=8.5$ Hz, ¹H), 5.10 (s, ²H), 5.22 (dd, $J=4.5, 11$ Hz, ¹H), 4.43 (m, ¹H), 2.97 (s, ³H), 1.82 (m, ¹H), 1.59 (m, ²H), 1.45 (m, ²H), 1.35 (m, ⁹H), 1.23 (m, ¹H), 0.86 (m, ¹²H); ¹³C NMR (CDCl₃, 125 Hz) δ (ppm): 173.96 (¹C), 171.31 (¹C), 155.57 (¹C), 135.65 (¹C), 128.71 (¹C), 128.59 (¹C), 128.26

(^1C), 128.08 (^2C), 79.42 (^1C), 66.81 (^1C), 55.29 (^1C), 49.14 (^1C), 42.85 (^1C), 37.40 (^1C), 31.66 (^1C), 28.35 (^3C), 25.05 (^1C), 24.65 (^1C), 23.39 (^1C), 23.26 (^1C), 21.90 (^1C), 21.30 (^1C). MS (ESI) m/z : 449.3 $[\text{M} + \text{H}]^+$, 466.5 $[\text{M} + \text{NH}_4]^+$, 471.6 $[\text{M} + \text{Na}]^+$.

Cell cultures

The human hepatoma BEL-7402 cells, breast cancer MCF-7 cells, human cervical epithelial carcinoma HeLa cells, hepatoma HepG2 cells, and human lung carcinoma A549 cells were obtained from the Department of Pathology of

Fig. 1



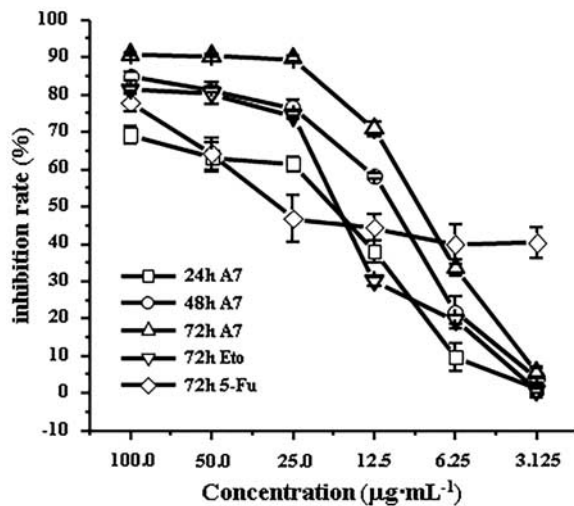
The chemical synthesis of novel leucine dipeptide benzyl ester derivatives. (a) The chemical structures of galaxamide. (b) The chemical structures of E1–E6. E1–E3 are isomers of Boc-Leu and E4–E6 are isomers of Leu-Bn. (c) A schematic representation of the strategies for the condensation reactions. (d) The chemical structures of A1–A7: A1, *N*-tertbutyl-L-leucine-*N*-methyl-L-leucinebenzyl; A2, *N*-tertbutyl-L-leucine-L-leucinebenzyl; A3, *N*-methyl-tertbutyl-L-leucine-L-leucinebenzyl; A4, *N*-tertbutyl-D-leucine-*N*-methyl-L-leucinebenzyl; A5, *N*-tertbutyl-L-leucine-*N*-methyl-D-leucinebenzyl; A6, *N*-methyl-tertbutyl-L-leucine-*N*-methyl-L-leucinebenzyl; A7, *N*-tertbutyl-D-leucine-*N*-methyl-D-leucinebenzyl.

Table 1 The IC₅₀ values of A1–A7 against human cancer cell lines

Compounds	IC ₅₀ (μg/ml)				
	HepG2	MCF-7	Bel-7402	HeLa	A549
5-FU	29.43 ± 2.31	1.10 ± 0.11	16.89 ± 0.76	2.13 ± 0.31	5.47 ± 0.28
A1	15.56 ± 1.03	17.32 ± 0.98	11.56 ± 1.20	> 100	> 100
A2	> 100	> 100	> 100	> 100	> 100
A3	> 100	> 100	> 100	> 100	> 100
A4	8.36 ± 0.47	12.04 ± 0.81	9.16 ± 0.35	> 100	> 100
A5	8.46 ± 0.26	12.73 ± 0.94	9.74 ± 0.78	> 100	> 100
A6	8.09 ± 0.33	8.84 ± 0.31	15.98 ± 1.01	10.7 ± 0.69	8.09 ± 0.34
A7	4.57 ± 0.19	6.33 ± 0.22	6.17 ± 0.39	> 100	> 100

5-FU, 5-fluorouracil.

Fig. 2



A7 treatment reduces tumor cell proliferation. HepG2 cells were incubated with different concentrations of A7 for 24, 48, and 72 h, and cell proliferation was determined using the MTT assay. Cells treated with Eto and 5-fluorouracil (5-FU) for 72 h were used as a control. The experiments were repeated three times. Data are presented as mean ± SD, $N=4$.

Jinan University (Guangzhou, China). The cells were cultured in RPMI-1640 medium (GIBCO, Grand Island, New York, USA) containing 10% neonatal bovine serum, 100 U/ml penicillin, and 100 μg/ml streptomycin. The cells were cultured at 37°C in a 5% CO₂, 95% air incubator, and fed every 2–3 days.

Cell proliferation assay

Cells in the logarithmic growth phase were harvested and seeded at a density of 4×10^4 cells/ml in 96-well plates (Costar, Cambridge, Massachusetts, USA) overnight. The stock solutions of synthesized peptides were dissolved in DMSO at concentrations of 25 mg/ml. When used, the stock solutions were doubly diluted from 100.0 to 3.125 μg/ml by RPMI-1640 medium containing 3% neonatal bovine serum. After treating the cells with various concentrations of the compounds for 72 h, the cytotoxicity of the compounds was determined by the MTT (Sigma, St Louis, Missouri, USA).

Cell cycle analysis

HepG2 cells were seeded in a six-well plate at a density of 1×10^6 cells/ml. After exposure to drugs, the cells were harvested by centrifugation, fixed with ice-cold 75% ethanol, and then resuspended in binding buffer. The cells were subsequently treated with RNase A for 30 min and stained with propidium iodide (100 μg/ml) at 37°C for 30 min in the dark. The stained cells were then analyzed by a flow cytometry system (Coulter Epics Elite, Beckman Coulter, California, USA). The percentage of cells in sub-G1 phase, G1 phase, S phase, and G2 phase was analyzed using standard ModiFit (Verity Software House, Topsham, Maine, USA) and CellQuest software programs (BD Biosciences, San Jose, California, USA).

Apoptosis assay

The cells were treated with various concentrations of A7 (0, 6.25, 12.5, and 25.0 μg/ml) for 24 h or with a fixed concentration of A7 (12.5 μg/ml) for different durations of time (0, 12, 24, or 48 h). After collecting and washing with PBS, the cells were resuspended in 500 μl of Annexin-V binding buffer. After adding Annexin-V-FITC/PI, cells were incubated in the dark for 15 min, acquired on a flow cytometry system, and analyzed using CellQuest software (WinMDI 2.9; BD Biosciences, San Jose, California, USA). The fraction of the cell population in different quadrants was analyzed using quadrant statistics.

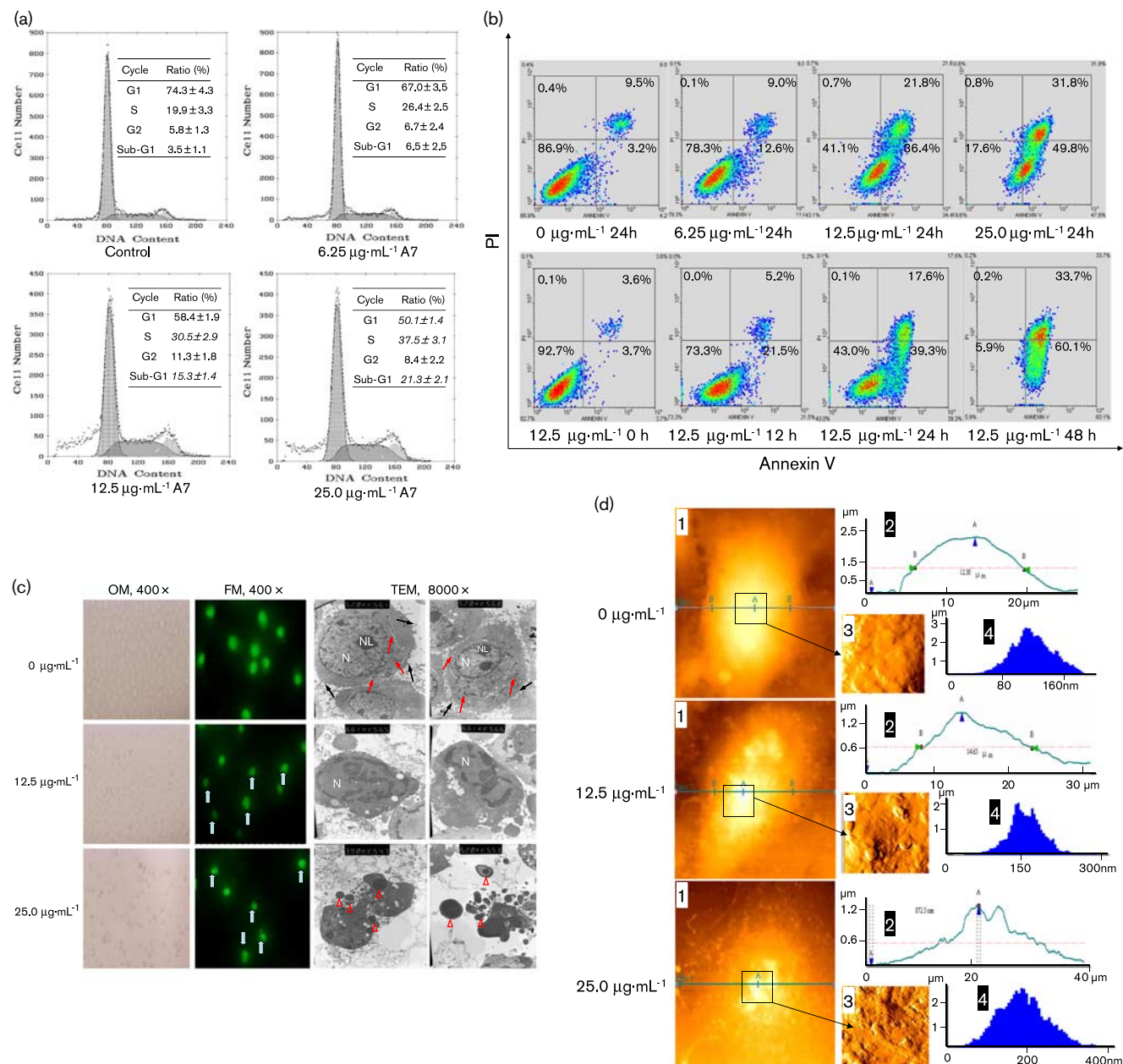
Evaluation of morphological changes of HepG2 cell by atomic force microscopy

HepG2 cells were treated with A7 (0, 12.5, and 25.0 μg/ml) for 24 h and subsequently fixed with 2.5% glutaraldehyde for 30 min at 4°C. The cells were then washed twice with cold PBS, air-dried, and observed under an atomic force microscope (Thermo Microscopes, Thermo Scientific, Waltham, Massachusetts, USA).

AO staining of the nuclei of A7-treated HepG2 cells

HepG2 cells were treated with A7 (0, 12.5, and 25.0 μg/ml) for 24 h. Then, the cells were collected, washed with PBS, and resuspended in 1 ml acridine orange (100 μg/ml acridine orange in PBS). After incubation for 15 min, the cells were examined under a fluorescence microscope (400-fold amplification) (Nikon, Tokyo, Japan).

Fig. 3



A7 induces cell cycle arrest and apoptosis. (a) The cell cycle distribution. Number CICCPS in bold and italics correspond to significant variations compared with the control. (b) Annexin-V/PI staining for apoptotic cells. Numbers in bold correspond to significant variations compared with the control. (c) Morphological observations of apoptotic cells. Apoptotic nuclei (blue arrows), microvilli (black arrows), rough endoplasmic reticulum and mitochondria (red arrow), nuclei (N), nucleolus (NL), and apoptotic body (hollow triangles) are indicated. (d) Atomic force microscopy (AFM) observation. Subpanel 1 shows the topological morphology of a single representative cell, bar: 1 mm. Subpanel 2 shows the line profile of subpanel 1 along the A and B labeled line. Subpanel 3 shows the ultrastructure of the cell membrane surface zoomed from the left images, box bar: 100 nm. Subpanel 4 shows the histogram of the particles of subpanel 3. CICCPS, carbonyl cyanide-*m*-chlorophenylhydrazide; PI, propidium iodide.

Transmission electron microscopy of HepG2 cells

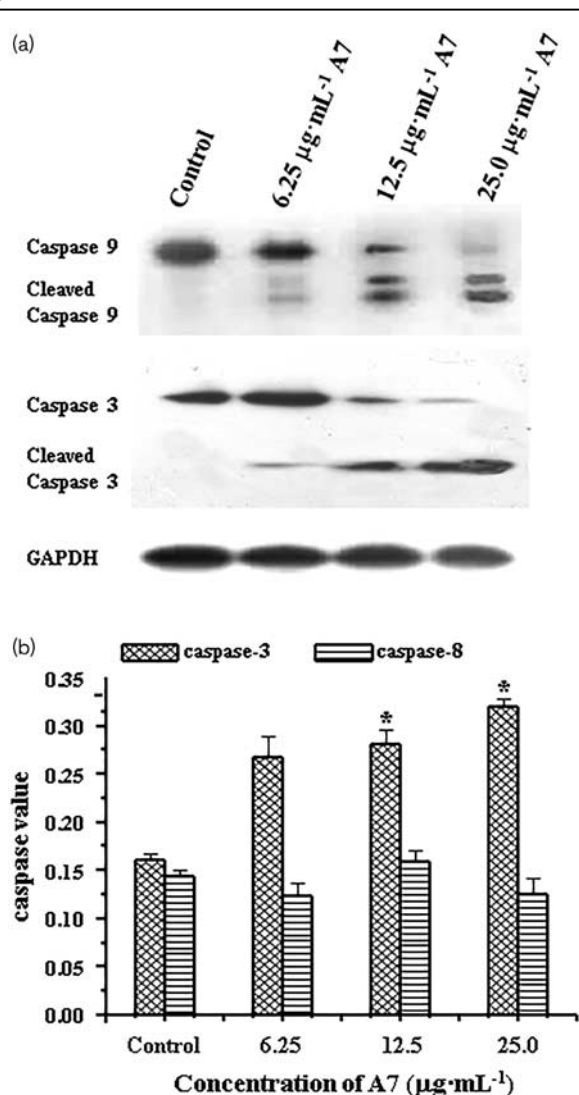
HepG2 cells were treated with 0, 12.5, or 25.0 µg/ml of A7 for 24 h. The cells were harvested, washed twice with cold PBS, and fixed with 2.5% glutaraldehyde in 0.1 mol/l PBS (pH 7.2) at 4°C. Then, the cells were postfixed with osmium tetroxide, dehydrated in an ethanol series, and embedded in epoxy resin. After staining with uranium

tetracetate and lead citrate, the cells were examined by JEM-100CXII transmission electron microscopy (Jeol Ltd, Tokyo, Japan).

Western blotting assay

Cells treated with 6.25–25.0 µg/ml of A7 for 24 h were lysed in lysis buffer (Beyotime Institute of

Fig. 4



Activation of the caspase cascade. (a) Western blots were performed to detect cleaved caspase-9 and caspase-3. (b) Colorimetric assay to detect the total activity of caspase-8 and caspase-3. Data are presented as mean \pm SD ($N=3$). * $P < 0.05$ versus the control group.

Biotechnology, Jiangsu, China) and centrifuged to collect cell extracts for electrophoresis. Proteins (50 μg) from samples were resolved on 10% SDS-polyacrylamide gels and transferred to epolyvinylidene difluoride membranes. After blocking with 5% nonfat milk, the membranes were probed with mouse anti-human-caspase monoclonal antibodies (Cell Signaling Technology, Boston, Massachusetts, USA) and a rabbit anti-GAPDH polyclonal antibody (Santa Cruz Biotechnology, Santa Cruz, California, USA). They were subsequently probed with peroxidase-conjugated secondary antibodies (KPL, Gaithersburg, Maryland, USA). Detection was carried out using the SuperSignal West Pico kit (Pierce Biotechnology, Rockford, Illinois, USA).

Total caspase activity assays

HepG2 cells (1×10^6 cells/ml) were harvested and washed twice with PBS. The cell lysate was incubated with the colorimetric substrate of caspase-8 or caspase-3 in a 96-well plate at 37°C for 4 h in a CO₂ incubator. Absorbance at 405 nm was determined by reading the plate with a microplate reader. Activities of caspase-8 and caspase-3 were expressed as the optical density value.

Intracellular Ca²⁺ concentration and mitochondrial membrane potential

Following appropriate treatment, the cells were collected by centrifugation, washed, and incubated at 37°C with Fluo-3 AM for 40 min or rhodamine-123 for 20 min. The cells were then washed three times with cold PBS. The intracellular Ca²⁺ concentration and the mitochondrial membrane potential ($\Delta\Psi_m$) were measured by flow cytometry. Carbonyl cyanide-*m*-chlorophenylhydrazone (Acros Organics, Geel, Belgium) was used as a positive control. The results were analyzed using Orig. 6.0 software (OriginLab Corporation, Northampton, Massachusetts, USA).

Statistical analysis

Data are presented as mean \pm SD. Comparisons between groups were performed using the analysis of variance test. Values of P less than 0.05 were considered to be statistically significant.

Results

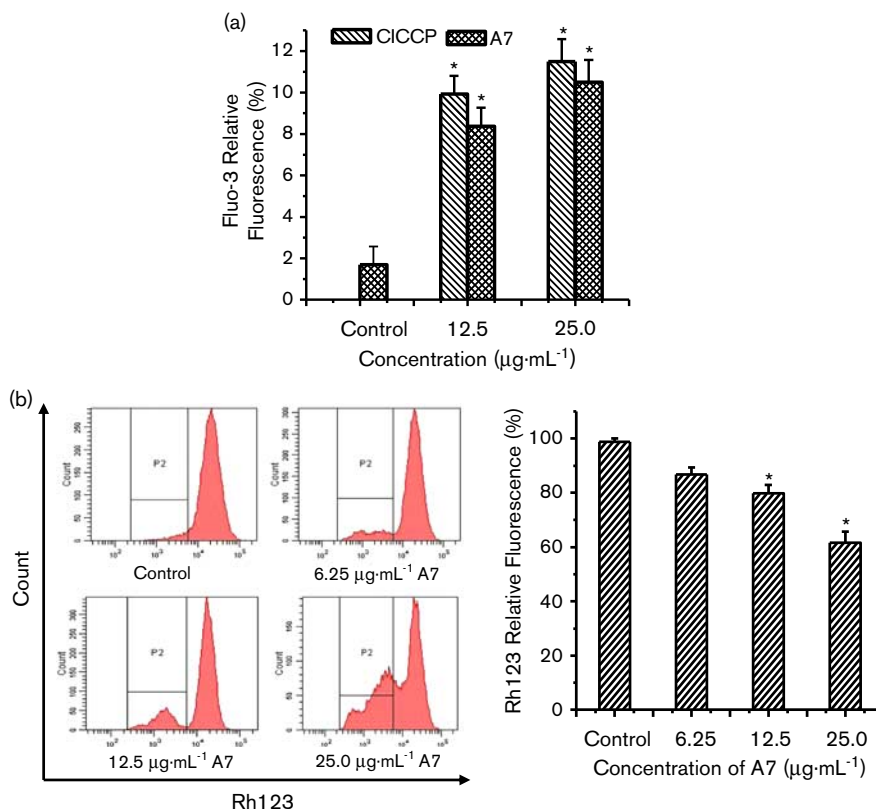
Design and synthesis of novel leucine dipeptide benzyl ester derivatives

To screen for leucine dipeptides with antitumor activity, we first designed six leucine derivatives (E1–E6), which were different from each other in the benzyl (Bn) or tert-butyloxycarbonyl (Boc) protective groups, the methyl group in amido, and D/L stereochemistry (Fig. 1b). Previously, we synthesized A1, *N*-tertbutyl-L-leucine-*N*-methyl-L-leucinebenzyl, by coupling E5 and E1 [9]. In the present study, six novel leucine dipeptide benzyl ester derivatives (A2–A7) were designed and synthesized by alternatively using E1–E3 and E4–E6 for condensation reactions (Fig. 1c and d). The three-dimensional conformation of A7 was studied by X-ray crystallographic analysis, which confirmed that this compound was not racemized during chemical synthesis (Supplementary Fig. S1, Supplemental digital content 1, <http://links.lww.com/ACD/A251> and Fig. S2, <http://links.lww.com/ACD/A252>).

Antitumor activity of A1–A7 in human cancer cells

The anticancer activity of the seven compounds was investigated *in vitro* on HepG2, MCF-7, Bel-7402, HeLa, and A549 cells (Table 1). The well-known anticancer chemotherapy drug 5-fluorouracil (5-FU) was used as a control. Antitumor activity was observed for all the compounds, except for A2 and A3, which showed no

Fig. 5



Disturbance in intracellular Ca^{2+} concentration and mitochondrial membrane potential ($\Delta\psi$). (a) Fluo-3 AM staining for the level of intracellular Ca^{2+} concentration. Data are presented as mean \pm SD ($N=3$). * $P < 0.01$ versus the control. (b) Rh123 staining for changes in the mitochondrial membrane potential ($\Delta\psi$). The left panel shows the fluorescence histograms of a representative test. Data are presented as mean \pm SD in the right panel. * $P < 0.05$ versus the control. The mean fluorescence for control cells was artificially set as 100.

effect on either of the five tumor cell lines. These two compounds lack a methyl group in the amido of Bn-Leu. These results suggested that the methyl-*N* in leucine is crucial for the antitumor activity of these leucine dipeptides, which is consistent with a previous report on compounds with methyl-*N* have antitumor activity [10]. In addition, we also found that when one of the protection groups (Boc or Bn) was removed, all of the compounds lost their antiproliferation activity (data not shown). A6 effectively inhibited the proliferation of all five cell lines, with an IC_{50} ranging from 8.09 to 15.98 $\mu\text{g}/\text{ml}$, which is comparable to that of 5-FU. Compounds A1, A4, A5, and A7 were selectively active against HepG2, MCF-7, and Bel-7402. These five compounds are different *D/L* stereomers and all of them have a methyl group in the amido of Bn-Leu. Among all the compounds tested, A7, the only stereomer condensed by double *D*-Leu, showed the highest antitumor cell activity, which was comparable to that of galaxamide. Therefore, this compound was selected for more detailed studies.

We tested the in-vitro activity of A7 on HepG2 cells with a wider dose range and various exposure durations

of exposure, which showed that A7 had a significant inhibitory effect on cell growth and viability in a time-dependent and concentration-dependent manner (Fig. 2). The IC_{50} values were 19.35 $\mu\text{g}/\text{ml}$ (24 h), 11.08 $\mu\text{g}/\text{ml}$ (48 h), and 4.78 $\mu\text{g}/\text{ml}$ (72 h), respectively. At the 72 h time-point, the IC_{50} values of 5-FU and etoposide (Eto), two traditional anticancer drugs that were used as controls, were 29.43 and 18.01 $\mu\text{g}/\text{ml}$, respectively. Thus, A7 is a promising antitumor compound, and its strong tumor-inhibitory effect led us to study its potential mechanism of action.

A7 inhibits cancer cells by cell cycle arrest and apoptosis induction

To unravel the potential mechanisms of the tumor-inhibitory effect of A7, HepG2 cells were treated with 6.25, 12.5, and 25.0 $\mu\text{g}/\text{ml}$ of A7 for 24 h and subjected to flow cytometry analysis for cell cycle distribution (Fig. 3a). Cells that arrested in the S phase increased from 19.9 ± 3.3 to 26.4 ± 2.5 , 30.5 ± 2.9 , and $37.5 \pm 3.1\%$, respectively. This was associated with a concomitant decrease in the percentage of G1 cells. The fraction of cells in the sub-G1 phase, a feature of nuclear apoptosis,

also increased from 3.5 ± 1.1 to 6.5 ± 2.5 , 15.3 ± 1.4 , and $21.3 \pm 2.1\%$ for the three doses of A7, respectively. In addition, the population of Annexin-V positive/propidium iodide-negative cells increased significantly in a time-dependent and dose-dependent manner, which suggested the induction of early apoptosis (Fig. 3b). Morphological observation detected marked changes that are typical to cells undergoing apoptosis, including loss of focal adhesion (Fig. 3c, panel a), nuclear condensation (Fig. 3c, panel b), margination, aggregation, and condensation of nuclear chromatin (Fig. 3c, panel c). When observed under an atomic force microscope, untreated cells showed features common to cancer cells, with an average cell height of $2.72 \pm 0.09 \mu\text{m}$ and a cell diameter of $12.30 \pm 0.21 \mu\text{m}$ (Fig. 3d). Cells cultured in the presence of A7 for 24 h showed a dose-dependent decrease in cell height together with an enlarged cell diameter. These findings indicated that A7 induced apoptotic volume decrease, which is an early prerequisite to apoptosis. Taken together, these results suggest that A7 inhibited the proliferation of cancer cells by inducing cell cycle arrest and apoptosis.

A7 induced cleavage of caspase-9 and caspase-3 in HepG2 cells

After treatment of HepG2 cells with different concentrations for 24 h, A7 upregulated levels of cleaved caspase-9 and caspase-3 in a concentration-dependent manner (Fig. 4a). Treatment of HepG2 cells with $6.25 \mu\text{g/ml}$ of A7 was sufficient to induce the cleavage of caspase-9. The amount of cleaved caspase-9 increased gradually with increasing A7 concentration. A similar effect of A7 was also observed on caspase-3. Colorimetric assay also detected a dose-dependent increase in the total level of caspase-3 upon A7 treatment, but no change was found for caspase-8 (Fig. 4b). These results support the idea that A7 acts as an antitumor agent by inducing cell apoptosis.

A7 alters intracellular Ca^{2+} concentrations and mitochondrial membrane potential ($\Delta\psi$)

HepG2 cells were treated with an increasing dose of A7 for 24 h, followed by cytofluorometric analysis to study Ca^{2+} release and $\Delta\psi$. Exposing the cells to 12.5 and $25.0 \mu\text{g/ml}$ of A7 increased the intracellular Ca^{2+} level by more than four times, and the same tendency was also observed for cells treated with cyanide-*m*-chlorophenylhydrazone (Fig. 5a). This was accompanied by a dose-dependent decrease in $\Delta\psi$ (Fig. 5b), which indicated that A7 increased intracellular Ca^{2+} levels and decreased the mitochondrial membrane potential. This result served as evidence of the effect of A7 on apoptosis induction.

Discussion

Naturally cyclic peptides are exceptionally resistant to denaturing and digestion. They function mainly as toxins or antimicrobial substances *in vitro* and have been used as scaffolds, precursors, and lead compounds for drug

design [11]. Although the cyclic penta-leucine-peptide, galaxamide that exhibited potent antineoplastic activity was successfully synthesized in our previous study, we are still challenged by the low yield and poor purity of galaxamide. In this study, we designed and synthesized a series of leucine homo-oligopeptides and identified compounds that were biologically active against tumors. So far, oligopeptides that have shown biological activities are almost all hetero-oligomers, and the shortest anticancer peptide compound in clinical trials is a tripeptide with an aromatic amino-acid residue (Tyr) with a functional benzene ring [12]. Here, we have shown that homo-oligopeptides of aliphatic and nonpolar amino acids were also bioactive against tumor cells. In addition, one leucine homodipeptide, A7, showed antineoplastic effects comparable to 5-FU and galaxamide. To our knowledge, A7 is the shortest homo-oligopeptide, and this is the first report that a linear homo-oligopeptide showed strong antitumor activity through apoptosis induction.

Generally, chemical modification of primary peptides has been used to improve the efficiency and therapeutic potential. One of the most frequently used strategies for such modification is to replace amino groups with other functional groups [13]. Another typical method is to incorporate a side-chain-modified amino-acid residue or other amino-acid analogs, such as D-amino acid, β -amino acid, and *N*-methylated amino acid [14]. Introduction of these modified amino acids into natural peptides usually exerts noticeable effects in their biological activities. Moreover, modification of marine cyclic peptides using special amino acid and nonamino acid fragments has been found to highly improve their bioactivities and makes them better lead compounds for potential application [15]. In our study, substitution of Bn-Leu with an *N*-methylated one was crucial for the antineoplastic activity of the dipeptide product. Dipeptide derivatives without this modification (A2 and A3) showed no inhibitory effects on tumor cells (Table 1). This might explain the widest antitumor spectrum of A6, which was condensed with two *N*-methylated leucines. In addition, D/L stereochemistry also affected the antitumor properties of the leucine dipeptide derivatives; D-leucine was beneficial over L-leucine. This might be because of the fact that human cells typically utilize L-amino acids for protein synthesis, and D-amino acids are produced by post-translational modification of proteins, which are found in bacteria and some marine organisms [16]. Thus, it is conceivable that replacing the two L-leucines in A6 with D-leucines will generate a new dipeptide with higher antitumor activity.

Cancer cells usually show an elevated threshold for apoptosis and defects in apoptosis pathways. Peptides that can induce apoptosis in cancer cells are considered prime candidates for the development of novel antitumor drugs. Many naturally derived peptides have been proven to exert their antiproliferative activity through

apoptosis induction [17]. In our study, in the presence of A7, atomic force microscopy observed apoptotic volume decrease, which is considered to be an early prerequisite to apoptosis that precedes key biochemical hallmarks of apoptosis. The apoptosis-induction effect of A7 was validated by several approaches commonly used to study cells undergoing apoptosis. The superior tumor-inhibitory effect of A7 over traditional chemotherapy drugs (e.g. 5-FU and Eto) suggests that it may be a promising candidate for future application. The obvious selectivity of leucine dipeptides against different cell lines suggested the involvement of cell type-dependent mechanisms in their activity.

In HepG2 cells treated with A7, apoptosis was initiated by an increase in the intracellular calcium concentration. The two main routes to apoptosis are the extrinsic and intrinsic (mitochondrial) pathways. Both involve activation of the caspase cascade and subsequent cleavage of multiple intracellular substrates. Many cationic peptides, such as bovine lactoferricin, magainin II, and CAP18, have been shown to induce apoptosis through a mitochondria-dependent pathway [18]. We observed a disturbance in the mitochondrial membrane potential in cells exposed to A7, which suggested the influence of A7 on mitochondrial membrane integrity. In addition, cleavage of caspase-9 and caspase-3 was also detected in cells exposed to A7, which suggested that A7 might induce apoptosis through the mitochondrial pathway. We still do not know how A7 targets this pathway, and it seems difficult to generalize this mechanism to all the dipeptides that we synthesized.

Conclusion

Leucine dipeptide derivatives are biologically active against human cancers, with an effect that depends on tumor cell type. The *N*-methyl group in their chemical structure and the *D/L* conformation of the amino-acid residue are critical for their antitumor activity and provide opportunities for further peptide modification. They inhibit tumor cell proliferation through cell cycle arrest and apoptosis induction. The obvious strong antitumor effects of these compounds make them attractive as candidates for cancer therapy. Efforts are required to further improve their drug ability and understand the molecular mechanisms of their action.

Acknowledgements

The authors thank Dr. Jun Fan of Institute for Virus Research of Kyoto University for her critical review of this manuscript. This work was supported by grants from the National Natural Science Foundation of China (21672084

and 41506156), the Natural Science Foundation of Guangdong Province (2016A030310095), the Guangdong Provincial Science and Tech Project (2015A020211016), and the Guangzhou Industry-Academia-Research Collaborative Innovation Project (201604016009).

Conflicts of interest

There are no conflicts of interest.

References

- Weiner GJ. Building better monoclonal antibody-based therapeutics. *Nat Rev Cancer* 2015; **15**:361–370.
- Firer MA, Gellerman G. Targeted drug delivery for cancer therapy: the other side of antibodies. *J Hematol Oncol* 2012; **5**:70.
- Thakur R, Kini S, Kurkalang S, Banerjee A, Chatterjee P, Chanda A, et al. Mechanism of apoptosis induction in human breast cancer MCF-7 cell by Ruviprase, a small peptide from *Daboia russelii russelii* venom. *Chem Biol Interact* 2016; **258**:297–304.
- Catalano S, Leggio A, Barone I, De Marco R, Gelsomino L, Campana A, et al. A novel leptin antagonist peptide inhibits breast cancer growth in vitro and in vivo. *J Cell Mol Med* 2015; **19**:1122–1132.
- Bhutia SK, Maiti TK. Targeting tumors with peptides from natural sources. *Trends Biotechnol* 2008; **26**:210–217.
- Erez N, Zamir E, Gour BJ, Blaschuk OW, Geiger B. Induction of apoptosis in cultured endothelial cells by a cadherin antagonist peptide: involvement of fibroblast growth factor receptor-mediated signalling. *Exp Cell Res* 2004; **294**:366–378.
- Craik DJ. Chemistry. Seamless proteins tie up their loose ends. *Science* 2006; **311**:1563–1564.
- Xu WJ, Liao XJ, Xu SH, Diao JZ, Du B, Zhou XL, Pan SS. Isolation, structure determination, and synthesis of galaxamide, a rare cytotoxic cyclic pentapeptide from a marine algae *Galaxaura filamentosa*. *Org Lett* 2008; **10**:4569–4572.
- Liao XJ, Xu WJ, Xu SH, Dong FF. Benzyl 2-[[2-(tert-butoxycarbonylamino)-4-methylpentanoyl]methylamino]-4-methylpentanoate. *Acta Crystallographica Section E-Structure Reports Online* 2007; **63**:O3313–U4398.
- Caleta I, Kralj M, Marjanovic M, Bertosa B, Tomic S, Pavlovic G, et al. Novel cyano- and amidinobenzothiazole derivatives: synthesis, antitumor evaluation, and X-ray and quantitative structure-activity relationship (QSAR) analysis. *J Med Chem* 2009; **52**:1744–1756.
- Hili R, Rai V, Yudin AK. Macrocyclization of linear peptides enabled by amphoteric molecules. *J Am Chem Soc* 2010; **132**:2889–2891.
- Xiao ZY, Jia JB, Chen L, Zou W, Chen XP. Phase I clinical trial of continuous infusion of tyrosereleutide in patients with advanced hepatocellular carcinoma. *Med Oncol* 2012; **29**:1850–1858.
- Hamada Y, Shioiri T. Recent progress of the synthetic studies of biologically active marine cyclic peptides and depsipeptides. *Chem Rev* 2005; **105**:4441–4482.
- Hruby VJ. Peptide science: exploring the use of chemical principles and interdisciplinary collaboration for understanding life processes. *J Med Chem* 2003; **46**:4215–4231.
- Gruner SA, Locardi E, Lohof E, Kessler H. Carbohydrate-based mimetics in drug design: sugar amino acids and carbohydrate scaffolds. *Chem Rev* 2002; **102**:491–514.
- Pisarewicz K, Mora D, Pflueger FC, Fields GB, Mari F. Polypeptide chains containing D-gamma-hydroxyvaline. *J Am Chem Soc* 2005; **127**:6207–6215.
- Sato M, Sagawa M, Nakazato T, Ikeda Y, Kizaki M. A natural peptide, dolastatin 15, induces G2/M cell cycle arrest and apoptosis of human multiple myeloma cells. *Int J Oncol* 2007; **30**:1453–1459.
- Mader JS, Richardson A, Salsman J, Top D, de Antueno R, Duncan R, Hoskin DW. Bovine lactoferricin causes apoptosis in Jurkat T-leukemia cells by sequential permeabilization of the cell membrane and targeting of mitochondria. *Exp Cell Res* 2007; **313**:2634–2650.